Available online at www.sciencedirect.com
ScienceDirect
Trans. Nonferrous Met. Soc. China 35(2025) 602−612
Transactions of Nonferrous Metals Society of China
www.tnmsc.cn

# Recovery of copper and cobalt from waste rock in Democratic Republic of Congo by gravity separation combined with flotation

Qing-qing WANG[1,2], Lei SUN[1,2], Yang CAO[1,2], Xin WANG[1,2],
Yi QIAO[1,2], Mei-tao XIANG[1,2], Guo-bin LIU[1,2], Wei SUN[1,2]

1. School of Minerals Processing and Bioengineering, Central South University, Changsha 410083, China;
2. Key Laboratory of Hunan Province for Clean and Efficient Utilization of Strategic Calcium-containing Mineral Resources, Central South University, Changsha 410083, China

Received 22 May 2023; accepted 29 January 2024

**Abstract:** Copper and cobalt were recovered from SICOMINES mining waste rock in the Democratic Republic of Congo. The process mineralogy of the samples was analyzed using scanning electron microscopy and energy dispersive spectroscopy. The results showed that copper minerals exhibited various forms and uneven particle sizes, while cobalt existed in the form of highly dispersed asbolane, and large amounts of easily slimed gangue minerals were filled in the samples, making it difficult to separate copper and cobalt minerals. The particle size range plays a decisive role in selecting the separation method for the copper−cobalt ore. Gravity separation was suitable for particles ranging from 43 to 246 μm, while flotation was more effective for particles below 43 μm. After ore grinding and particle size classification, applying a combined gravity separation (shaking table)−flotation method yielded concentrated minerals with a copper recovery of 72.83% and a cobalt recovery of 31.13%.

**Key words:** copper−cobalt waste ore; process mineralogy; pre-classification; flotation; gravity separation

## 1 Introduction

As strategic metals for the Democratic Republic of the Congo (DRC), copper and cobalt play an important role in the country's GDP since revenues from their exports account for approximately 20% [1−3]. With the continuous extraction of copper−cobalt ores, high-grade and easily processable ores were selectively targeted for development [4], while due to economic and technical constraints, highly oxidized and low-grade ores were selectively discarded [5−8]. These refractory ores were regarded as waste ores, and their storage resulted in significant resource depletion and extensive land utilization, with significant security and environmental risks [9−12]. With the rapid proliferation of electric vehicles powered by renewable energy as a sustainable transportation means for combating climate warming, the demand for cobalt and copper metals has significantly increased [13−15]. Therefore, it is crucial to economically and sustainably utilize these resources.

Currently, the primary methods employed for the beneficiation of copper−cobalt minerals in the DRC were gravity separation and flotation [16]. Gravity separation relies on mass, volume, and shape properties to separate mineral particles in a liquid medium. Heavy medium separation (HMS) has been used in Katanga to pre-separate copper−cobalt ore from gangue minerals. HMS technology was particularly prominent in discarding talc and dolomite gangue minerals. Flotation was commonly

**Corresponding author:** Lei SUN, Tel: +86-13687361828, E-mail: sunlei@csu.edu.cn
DOI: https://doi.org/10.1016/S1003-6326(24)66702-6

regarded as a precursor to hydrometallurgical or pyrometallurgical treatment, especially in dealing with oxidized Cu−Co ores with relatively complex mineralogical characteristics [17]. The sulfidation flotation was the most prevalent method for copper−cobalt oxidized ores [18,19]. The sulfidation process can be affected by various factors, such as using different sulfidization agents, the dosage of sulfidization agents, and using different collectors after sulfidation [20−24]. Sulfidization was critical in enhancing the recoveries of copper−cobalt [25,26]. In the Katanga Cu−Co industry, surface sulfidation was preferred, followed by actual flotation in treating malachite and heterogeneous ore.

Whether using the HMS or flotation method, their research objectives primarily focus on the easily separated copper sulfides and the simple composition of oxidized Cu−Co ores. In the DRC, copper and cobalt were predominantly sourced from oxidized ore deposits [27,28]. However, with the exhaustion of high-grade oxidized Cu−Co ores, researchers have shifted their focus toward low-grade disseminated ores [29,30]. Achieving satisfactory indexes through single flotation or gravity separation method poses significant challenges.

In this work, low-grade copper−cobalt waste ore in the DRC was focused on. Based on mineralogical analysis, the characteristics of mineral association, grinding fineness, and beneficiation methods and conditions, including gravity separation and flotation, were investigated. Their impact on the separation efficiency of copper−cobalt waste ore was assessed. An economically viable process for separating and utilizing copper−cobalt waste ore was proposed.

## 2 Experimental

### 2.1 Materials and reagents

The samples comprised waste ore accumulated at the SICOMINES Copper and Cobalt Mine in the DRC. The ore sample was crushed to less than 2 mm and thoroughly mixed to prepare a homogeneous sample. A 500 g subsample was subjected to the mineralogical characterization analysis. The remaining samples were used for shaking table and flotation experiments. Sodium hexametaphosphate and sodium sulfide were used as regulators. Sodium butyl xanthate was regarded as the flotation collector and terpineol as a frother. The analytical purity of all flotation reagents was above 99.5% and purchased from Macklin Biochemical Company (Shanghai, China).

### 2.2 Analysis methods

The mineral characteristics were investigated, including elements and composition of minerals, chemical compositions of copper and cobalt phases, mineral granularity distribution, mineral disseminated relationships and mineral liberation. The general mineral composition of the ore samples was analyzed by X-ray diffraction (X′Pert3 Powder, Malvern Panalytical, NL). The particle morphological analysis and overall chemical analysis were carried out using scanning electron microscopy (Helios 5UC, Thermo Fisher Scientific, USA) and energy dispersive spectroscopy (Helios 5UC, Thermo Fisher Scientific, USA).

### 2.3 Shaking table and flotation experiments

The mineral grinding process was performed in a XMQ conical ball mill with the size of *d*240 mm × 90 mm (Wuhan Exploring Machinery Plant, China) at a slurry concentration of 66%. The post-classification samples were carried out in the shaking table (Luoyang Zhongde Heavy Industry Co., China) and the flotation machine (Jinlin Prospecting Machinery Factory, Changchun, China). The optimum flushing water and inclination angle of the shaking table were determined.

## 3 Results and discussion

### 3.1 Process mineralogy analysis results of ore samples

#### 3.1.1 Element and mineral compositions of ore samples

The results from the ore sample multi-element analysis were given in Table 1. As can be seen, copper and cobalt were the useful elements in the ore sample with 1.01 wt.% and 0.0452 wt.%, respectively. However, the contents of nickel, lead, zinc, and silver were too low to be economically valorized. The main oxides observed in the gangue included silicon dioxide ($SiO_2$), calcium oxide (CaO), magnesium oxide (MgO), and aluminum oxide ($Al_2O_3$), with a total content of 74.50 wt.%. The XRD analysis results of raw ore samples were depicted in Fig. 1. The types and contents of the minerals in the sample were shown in Table 2. Copper minerals mainly included malachite, chalcocite, and chrysocolla, with small amounts of cuprite, tenorite, covellite, and cornetite. Occasionally, chalcopyrite, bornite, and native copper were found in copper minerals. As for cobalt, it was found in the sample only as asbolane. Hematite and minor magnetite amounts were also observed in the ore samples. The gangue minerals were mainly composed of quartz and dolomite, with mica, feldspar, and chlorite, with occasional calcite, apatite, and rutile as minor minerals.

3.1.2 Chemical phase and mineral size distribution

The results of mineralogical phase analysis for copper and cobalt in samples were depicted in Tables 3 and 4, respectively. Primary copper sulfides accounted for only 0.99% of the sample, whereas secondary copper sulfides accounted for 30.69%. 63.37% of free oxidized copper was mainly obtained from malachite and chrysocolla. Cobalt sulfide observed in the sample accounted only for 2.20% versus cobalt oxide, of which the proportion was as high as 86.35%. The remaining cobalt was distributed in gangue minerals. Consequently, the recovery of cobalt minerals through flotation can be challenging since cobalt oxide was mainly present as amorphous asbolane. The granularity distribution of minerals was related to the mineralogical characteristics of ground ore samples. The particle size cumulative curve of valuable minerals in the crushed sample was presented in Fig. 2. The copper and cobalt minerals

**Table 1** Results of chemical composition analysis of ore sample (wt.%)

| Cu | Co | S | TFe | P | $SiO_2$ | CaO |
|---|---|---|---|---|---|---|
| 1.01 | 0.0452 | 0.07 | 1.86 | 0.06 | 54.58 | 7.90 |
| MgO | $Al_2O_3$ | MnO | $Na_2O$ | $K_2O$ | C | LOI |
| 8.67 | 3.35 | 0.17 | 0.07 | 1.90 | 3.37 | 9.23 |

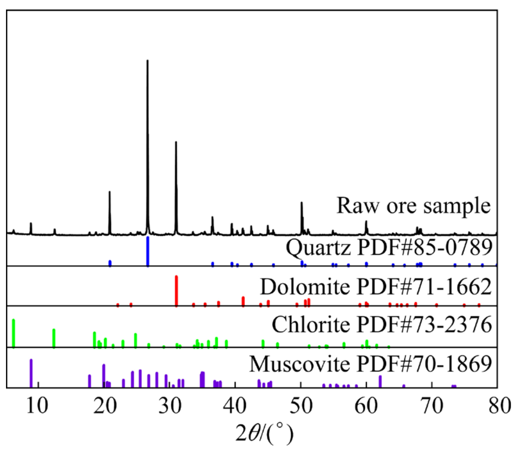


**Fig. 1** XRD pattern of raw ore sample

**Table 2** Types and contents of minerals in samples (wt.%)

| Quartz | Dolome | Mica | Malachite |
|---|---|---|---|
| 46.95 | 29.46 | 10.85 | 0.99 |

| Feldspar | Hematite | Chlorite |
|---|---|---|
| 4.18 | 1.15 | 4.86 |
| Chalcocite | Asbolae | Apatite |
| 0.36 | 0.30 | 0.29 |

| Chrysocolla | Tenorite | Chalcopyrite | Others |
|---|---|---|---|
| 0.16 | 0.05 | 0.04 | 0.36 |

**Table 3** Chemical phase analysis results of copper in samples

| Phase | Content/wt.% | Proportion/% |
|---|---|---|
| Primary copper sulfides | 0.01 | 0.99 |
| Secondary copper sulfides | 0.31 | 30.69 |
| Free copper oxide | 0.64 | 63.37 |
| Combined copper oxide | 0.03 | 2.97 |
| Native copper | 0.02 | 1.98 |

**Table 4** Chemical phases analysis results of cobalt in samples

| Phase | Content/wt.% | Proportion/% |
|---|---|---|
| Sulfide | 0.0011 | 2.20 |
| Oxide | 0.0430 | 86.35 |
| Cobalt contained gangue | 0.0057 | 11.45 |

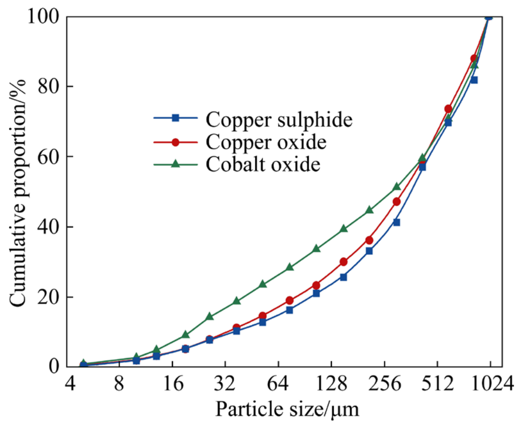


**Fig. 2** Particle size cumulative curves of valuable minerals in crushing sample

in the ore samples were composed of inhomogeneous disseminated particles from medium to fine size. For the particle size greater than 74 μm, the positive cumulative proportions of copper sulfide minerals, copper oxide minerals, and cobalt ores were 83.64%, 80.91%, and 71.63%, respectively. The inlay particle sizes of copper sulfide and copper mineral in the ore were similar.

3.1.3 Main minerals disseminated relationships

Chalcocite was revealed to be the main copper sulfide observed in samples, with a pale blue color in reflected light. Its distribution in the samples was irregular and varied with the particle size. As shown in Fig. 3, chalcocite typically occurs as subhedral to anhedral grains in agglomerate and fine-vein textures, with a grain size ranging from 10 to 150 μm. As for other copper sulfide minerals, including chalcopyrite, bornite, and covellite, their content was less than 0.05%. Chalcocite exhibited complex intergrowth relationships with other copper minerals, hematite and gangue minerals. In particular, chalcocite was closely associated with hematite, resulting in chalcocite−hematite aggregations.

Malachite was the most widely distributed copper mineral in the samples. Under transmitted light, it appeared as green particles, with an interference color slightly higher than gangue minerals such as quartz under reflected light and a grey-green internal reflection color. As illustrated in Fig. 4, malachite crystals appeared fine needle-shaped, fibrous, or leaf-shaped, aggregating in bundles, combs, or radials. Most malachite crystals were well-formed, with a small amount of disseminated chrysocolla. Some malachite appeared as fine irregular granules and fibrous textures, impregnated in gangue, with a grain size below 50 μm.

Asbolane was the main cobalt mineral observed in the samples. It was typically a secondary product formed by the weathering of basic and non-basic rocks containing cobalt found in the weathered crusts of such rocks. Asbolane was often associated with hematite but not closely linked with other copper minerals. It commonly appeared at the margins or intergranular spaces, partially filling hematite. As depicted in Fig. 5, scanning cobaltite crystals for cobalt elemental spectra reveals irregular and amorphous shapes, with extremely uneven distribution throughout the field of view. Asbolane was also distributed at edges of quartz, mica, and chlorite.

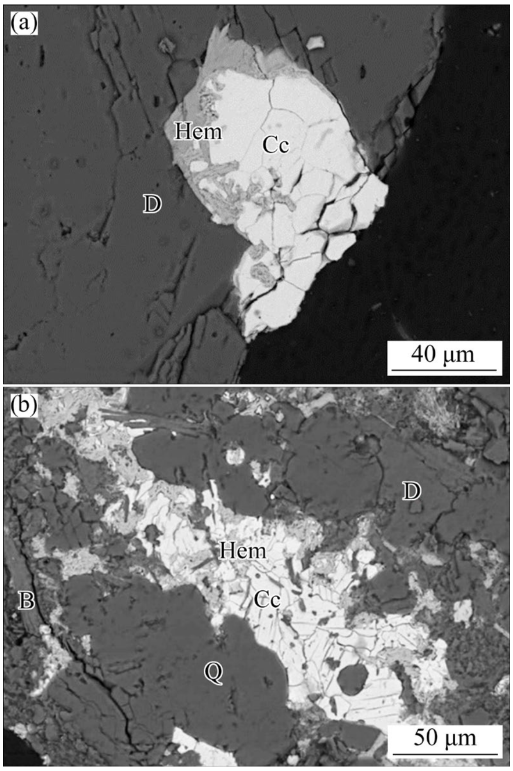


**Fig. 3** SEM images of assemblage of chalcocite and hematite intimate intergrowth along margin of dolomite and quartz (Cc: Chalcopyrite; Hem: Hematite; D: Dolomite; Q: Quartz; B: Mica): (a) Irregular massive chalcocite; (b) Fine-veined chalcocite

3.1.4 Main occurrence state of valuable metals and mineral liberation

Copper and cobalt were the main chemical elements of interest in the analyzed samples. The distribution equilibrium of copper and cobalt elements was estimated based on the contents of major minerals and spectral components of SEM. Figure 6 demonstrated that copper was mainly distributed in malachite and chalcocite, with distribution rates of 46.36% and 27.78%, respectively. A small amount of copper was found in chrysocolla and asbolane, with distribution rates of 5.51% and 5.42%, respectively. Cobalt was predominantly concentrated in amorphous asbolane, with a distribution rate as high as 81.77%. As shown in Table 5, under a grinding fineness of <74 μm, accounting for 70% of the total, the individual liberation degrees of copper and cobalt minerals were 74.86% and 54.67%, respectively. These results provided a detailed description of the

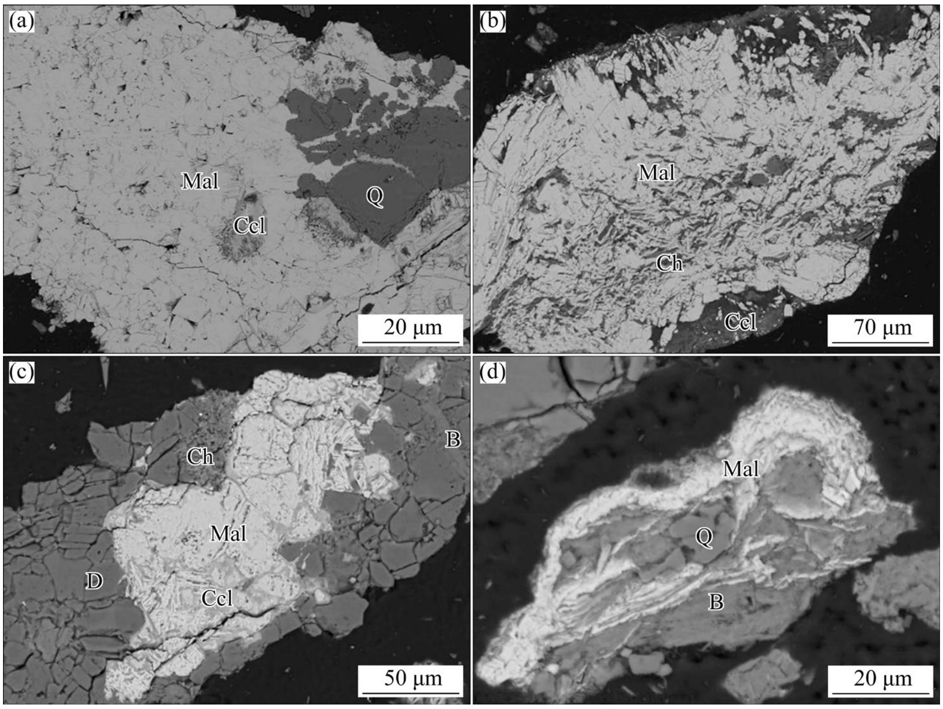


**Fig. 4** SEM images of irregular malachite closely associated with chrysocolla and quartz (Mal: Malachite; Ccl: Chrysocolla; D: Dolomite; Q: Quartz; B: Mica; Ch: Chlorite): (a) Needle-shaped malachite; (b) Disseminated malachite; (c) Leaf-shaped malachite; (d) Fibrous malachite

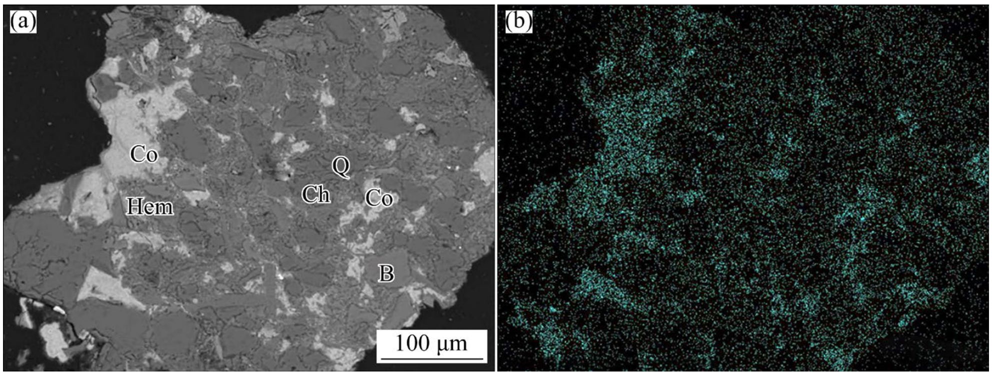


**Fig. 5** SEM images of asbolane highly dispersed throughout ore sample (Co: Asbolane; Hem: Hematite; Ch: Chlorite; Q: Quartz; B: Mica): (a) SEM image of disseminated asbolane; (b) Cobalt elemental mapping

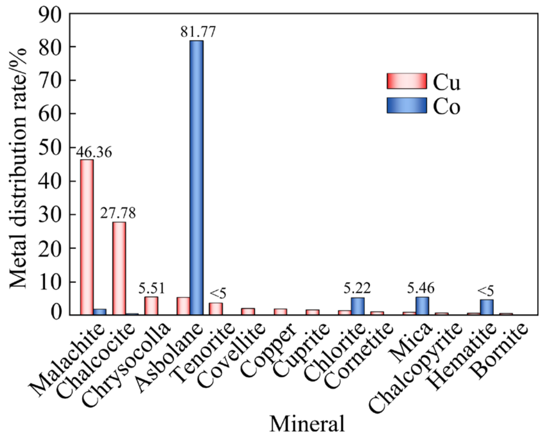


**Fig. 6** Elemental occurrence of Cu and Co in main minerals in samples

**Table 5** Liberation degrees of copper and cobalt minerals with grinding fineness of <74 μm accouting for 70% (%)

| Mineral | Monomer | Aggregate | | | |
|---|---|---|---|---|---|
| | | >3/4 | 3/4−1/2 | 1/2−1/4 | <1/4 |
| Copper minerals | 74.86 | 9.73 | 5.00 | 2.78 | 7.64 |
| Asbolane | 54.67 | 29.62 | 4.36 | 5.81 | 5.54 |

distribution of copper and cobalt in different minerals and the individual liberation degrees under specific grinding fineness conditions. These results offered valuable guidance for recovering copper and cobalt minerals in subsequent processes.

### 3.2 Shaking table and flotation experiment results

The feasibility of mineral separation can be approximately assessed by employing the following formula:

$$E=(\delta_2-\rho)/(\delta_1-\rho)$$

where $E$ represented the criterion value for the difficulty level of the gravity separation; $\delta_1$, $\delta_2$ and $\rho$ represented the specific density of light mineral, heavy mineral, and fluid medium, respectively. The criterion value $E$ could be divided into five grades, as shown in Table 6.

**Table 6** Difficulty level of gravity separation

| $E$ value | >2.5 | 2.5−1.75 | 1.75−1.5 | 1.5−1.25 | <1.25 |
|---|---|---|---|---|---|
| Difficulty level | Greatly easy | Easy | Medium | difficult | Greatly difficult |

The lower the $E$ value is, the greater the difficulty of separation is. In this ore sample, the primary valuable minerals and gangue minerals were malachite and quartz, with densities of 3600 and 2650 kg/m$^3$, respectively. The density of the separation medium, water, was assumed to be 1000 kg/m$^3$. The calculated $E$ value was 1.58, falling within the theoretically feasible range.

3.2.1 Effect of grinding fineness on shaking table performance

Before initiating the shaking table experiments, the ore samples underwent a grinding process. With the shaking table's operating parameters fixed at a horizontal slope of 2.0°, a stroke of 13 mm, a frequency of 305 r/min, and an ore feed concentration ranging from 20% to 30%, distinct zoning phenomenon was observed in the bed surface separation area. Consequently, under these unaltered conditions, we investigated the influence of grinding fineness on the recovery rates of copper and cobalt minerals in shaking table separation. As seen from Fig. 7, the recovery rates of copper and cobalt first increased before decreasing with an increase in the grinding fineness. The maximum recovery rate was achieved for a grinding fineness of 70%. However, copper and cobalt grades remained relatively stable across all grinding fineness levels, equivalent to the raw ore. The above results showed that the grinding samples directly enter the shaking table to beneficiate copper−cobalt ore. The separation effect was poor due to the uneven particle size. Indeed, the disturbance induced by flushing water resulted in the substantial loss of fine particles to the tailings. Meanwhile, particle size notably influences coarse particles' separation behavior. The combined impact of these factors renders the performance of shaking table separation relatively suboptimal, irrespective of the selected grinding fineness.

3.2.2 Effect of particle size on shaking table performance

Due to the uneven particle size distribution resulting from the grinding process, coarse and fine particles were intermixed. Adjusting the grinding fineness does not effectively improve the shaking table separation efficiency. Under grinding fineness conditions of 55% and 70%, the disparities in recovery rates and grades of copper and cobalt were not pronounced. However, at a grinding fineness of 70%, there was a significant increase in the content of particles with sizes <43 μm (refer to Fig. 8), which was proved to be detrimental to the effectiveness of shaking table separation. Consequently, further

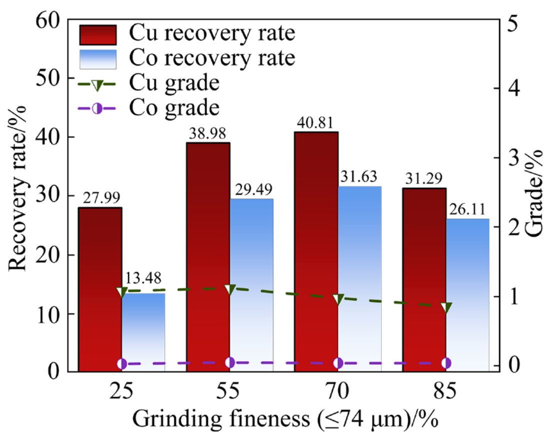


**Fig. 7** Effect of grinding fineness on shaking table concentrate

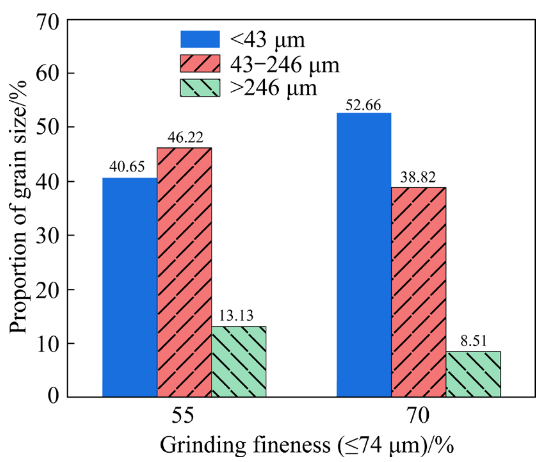


**Fig. 8** Proportions of different groups of graded products

investigations were conducted at a grinding fineness of 55%, specifically focusing on three particle size fractions: >246 μm, 43−246 μm, and <43 μm. The results of these shaking table separation tests were shown in Fig. 9.

As depicted in Fig. 9, the shaking table exhibited a specific separation effect for medium-fine particles, with copper grade and recovery rate reaching 7.05% and 54.91%, respectively, for particle sizes within the 43−246 μm range. For fine particle sizes (<43 μm), although the copper grade increased, the overall recovery rate remained below 10%. The cobalt occurred as amorphous minerals associated with the gangue minerals. The grade of cobalt barely changed and remained at about 0.5% in the whole range of particle sizes, revealing a poor recovery of cobalt minerals employing a shaking table. It can be concluded that the grinding sample was further graded by particle size to remove the uneven interference of the particle size and enabled the shaking table to effectively recover copper particles of medium to fine size.

To enhance overall copper and cobalt recovery, particles ranging from 43 to 246 μm were selected for shaking table classification. The flotation experiments were conducted on particles smaller than 43 μm and a blend of shaking table tailings.

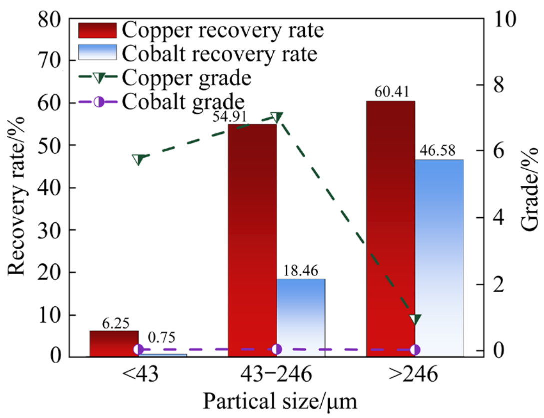


**Fig. 9** Effect of particle size on separation performance of shaking table

### 3.3 Flotation experiment results

In the flotation tests, the sulfide flotation method was employed. Sodium hexametaphosphate was used as a gangue mineral dispersant, while sodium sulfide was a surface sulfidizing agent for copper−cobalt oxide minerals. Sodium butyl xanthate was employed as the collector. Additionally, terpineol was utilized as a frothing agent for the pulp. The specific flotation process is delineated in Fig. 10. The impacts of the dosages of sodium hexametaphosphate, sodium sulfide, and sodium butyl xanthate on the separation of copper and cobalt minerals were depicted in Figs. 11, 12, and 13, respectively.

As shown in Fig. 11, with the gradual increase in the dosage of sodium hexametaphosphate from

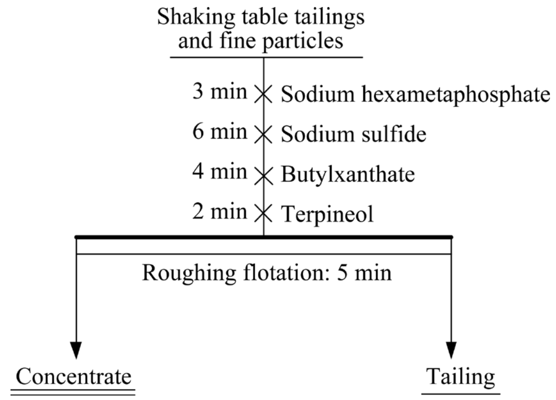


**Fig. 10** Rough flotation flowchart of shaking table tailing and fine particles

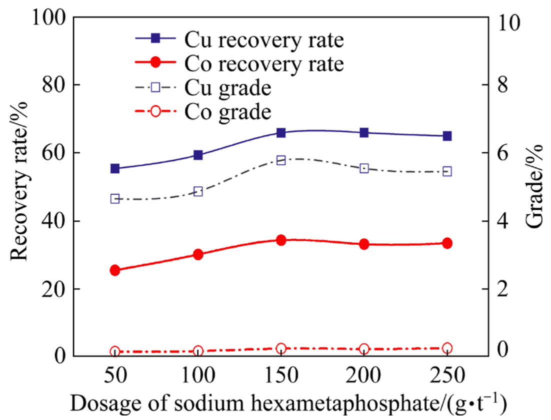


**Fig. 11** Effect of sodium hexametaphosphate dosage on speparation of copper and cobalt

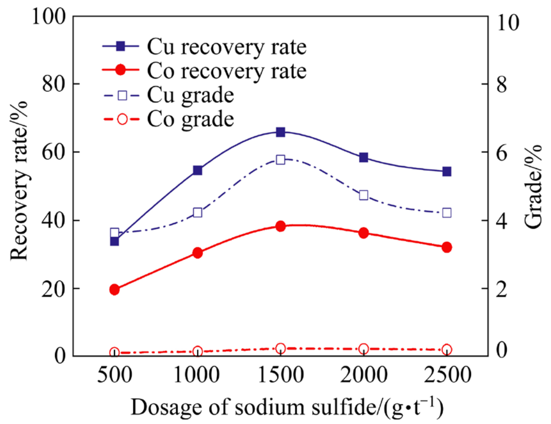


**Fig. 12** Effect of sodium sulfide dosage on separation of copper and cobalt

50 to 250 g/t, both the recovery rates and grades of copper and cobalt showed an ascending trend before reaching a state of stabilization. At a 150 g/t dosage, peak recovery rates were attained, with copper and cobalt achieving values of 65.84% and 34.32%, respectively, and copper grade reaching as high as 5.78%. Cobalt grade maintained a relatively low level over the entire range of reagent dosages, without exceeding 0.5%.

As illustrated in Fig. 12, when sodium sulfide dosage increased from 500 to 2500 g/t, recovery rates of copper and cobalt increased rapidly before decreasing. As the sodium sulfide dosage exceeded 1500 g/t, the competitive adsorption of the collector and excessive hydrogen sulfide ions on the surface of copper oxide led to the decreased copper recovery rate. The optimum dosage for copper recovery was 1500 g/t. As for the grades of metals, the copper reached its maximum for a sodium sulfide dosage of 1500 g/t when the cobalt grade barely changed whatever the sodium sulfide dosage.

As shown in Fig. 13, as the dosage of sodium butyl xanthate gradually increased, the recovery rates of copper and cobalt exhibited a sharp and pronounced upward trend, reaching 65.84% and 36.25%, respectively, at a dosage of 150 g/t. Beyond this dosage, the recovery rates of both metals stabilized. Concurrently, the copper grade exhibited an initial increase followed by a decline,

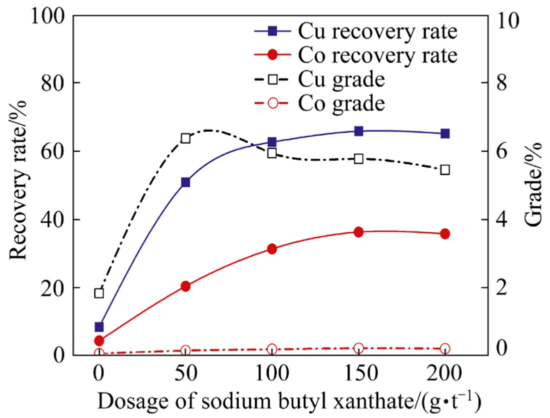


**Fig. 13** Effect of sodium butyl xanthate dosage on separation of copper and cobalt

while the cobalt grade remained relatively low. Considering all factors, the optimal dosage of sodium butyl xanthate is 150 g/t.

### 3.4 Combination of gravity separation and flotation

Experiments determined that the copper−cobalt waste ore was suitable for treatment using a combined gravity separation−flotation method. A grinding fineness of 55% was set, and the ore was subsequently classified into two particle sizes: <43 μm and >43 μm. The fraction of particles with sizes >43 μm was separated by the shaking table, while the fraction of <43 μm was mixed with shaking table tailings for flotation separation, as illustrated in Fig. 14. The

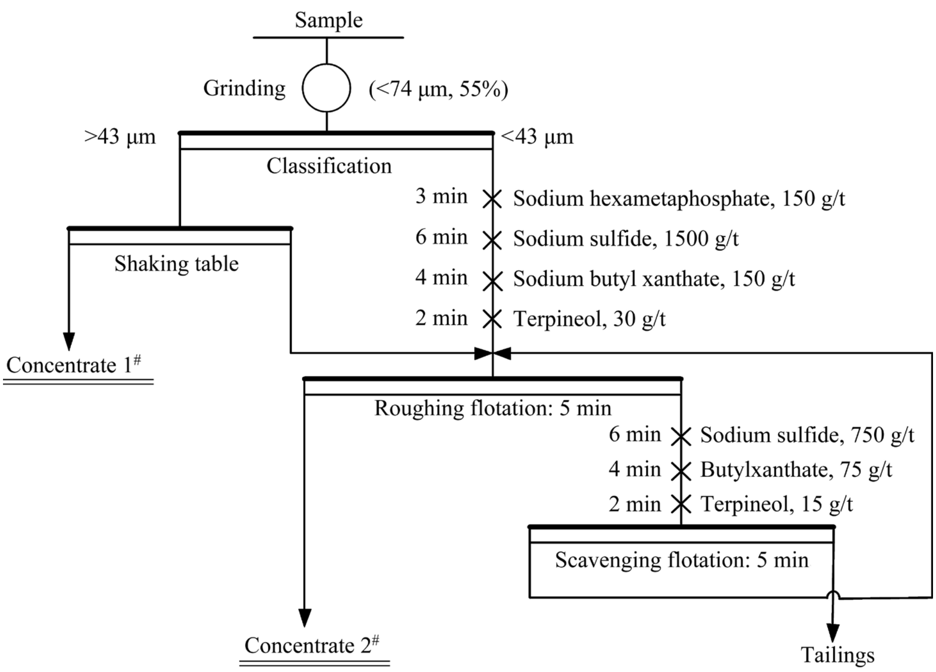


**Fig. 14** Experiment flowchart of combination of shaking table and flotation

results of Table 7 indicated that the shaking table concentrate yielded a copper grade of 5.84% and a cobalt grade of 0.07%, while the flotation concentrate achieved a copper grade of 4.87% and a cobalt grade of 0.13%. The final total recovery rates for copper and cobalt were 72.83% and 31.13%, respectively.

**Table 7** Experimental results of combination of shaking table and flotation (wt.%)

| Products | Yield | Recovery rate/% | | Grade/% | |
|---|---|---|---|---|---|
| | | Cu | Co | Cu | Co |
| Concentrate 1# | 4.81 | 27.78 | 6.75 | 5.84 | 0.07 |
| Concentrate 2# | 9.35 | 45.04 | 24.38 | 4.87 | 0.13 |
| Total concentrates | 14.16 | 72.83 | 31.13 | 5.19 | 0.11 |
| Tailings | 85.84 | 27.17 | 68.87 | 0.32 | 0.04 |
| Samples | 100 | 100 | 100 | 1.01 | 0.05 |

The obtained concentrate can be subjected to hydrometallurgical processing to prepare commercial-grade copper and cobalt. The sample was the copper−cobalt oxide concentrate, usually processed through a leaching−solvent extraction−electrowinning route. After the leaching of oxidized ore, copper was separated by solvent extraction, and some impurities such as iron, aluminum and manganese were removed by selective chemical precipitation before the cobalt recovery by precipitation with magnesia. The utilization of a combined shaking table and flotation approach provides several benefits, including the ability to achieve coarser grinding fineness which helps to in reduce sliming, as well as obtaine high-quality copper ores by using the shaking table as a pre-treatment step.

## 4 Conclusions

(1) The mineral composition of copper and cobalt waste ore in the SICOMINES mining area was complex and closely related. Copper minerals existed in various forms and uneven particle sizes. Cobalt was distributed in irregular amorphous asbolane. A large amount of easily slimed dolomite, mica and chlorite filled the sample, which might have deteriorated the efficiency of the separation process.

(2) In order to reduce the loss of copper and cobalt metals caused by sliming, ore samples were treated with coarse-grained and pre-classified to eliminate interference caused by uneven grain sizes. In the particle size range of 43−246 μm, the shaking table demonstrated excellent separation performance for copper ore grade and recovery rate, which could realize the effective recovery of copper minerals.

(3) Particles smaller than 43 μm were separated using the sulfide−xanthate flotation method, which employed sodium hexametaphosphate as a dispersant, sodium sulfide as an activator, and sodium butyl xanthate as a collector. This process effectively enriched the fine-grained copper minerals in the samples.

(4) The copper concentrate with a copper grade of 5.19% and copper recovery rate of 72.83% was obtained by a combined gravity separation−flotation method. As an associated mineral, cobalt was also effectively recovered with a recovery rate of 31.13%. The implemented process could effectively prevent overgrinding of samples and reduce slime formation. It provided a potential idea for the dispose of the waste rock accumulated during ore mining to maximize resource utilization and ensure environmental protection.

### CRediT authorship contribution statement

**Qing-qing WANG:** Investigation, Software, Writing – Original draft; **Lei SUN:** Methodology, Funding acquisition, Writing – Review & editing; **Yang CAO:** Investigation, Conceptualization, Software; **Xin WANG:** Investigation, Software; **Yi QIAO:** Investigation, Data curation; **Mei-tao XIANG:** Investigation, Methodology; **Guo-bin LIU:** Investigation; **Wei SUN:** Methodology, Conceptualization.

### Declaration of competing interest

The authors declare that they have no known competing financial interests or personal relationships that could have appeared to influence the work reported in this paper.

### Acknowledgments

The authors sincerely thank the National Key Research and Development Program of China (No. 2020YFC1909202), and the Major Science and Technology Program of Yunnan Province, China (No. 202202AB080012) for financial support.

## References


[1] SHENGO M L, KIME M B, MAMBWE M P, NYEMBO T K. A review of the beneficiation of copper-cobalt-bearing minerals in the Democratic Republic of Congo [J]. Journal of Sustainable Mining, 2019, 18(4): 226−246.

[2] GULLEY A L. One hundred years of cobalt production in the Democratic Republic of the Congo [J]. Resources Policy, 2022, 79: 103007.

[3] DEBERDT R. The Democratic Republic of the Congo (DRC)'s response to artisanal cobalt mining: The Entreprise Générale du Cobalt (EGC) [J]. The Extractive Industries and Society, 2021, 8(4): 101013.

[4] MEES F, MASALEHDANI M N N, DE PUTTER T, D'HOLLANDER C, VAN BIEZEN E, MUJINYA B B, POTDEVIN J L, VAN RANST E. Concentrations and forms of heavy metals around two ore processing sites in Katanga, Democratic Republic of Congo [J]. Journal of African Earth Sciences, 2013, 77: 22−30.

[5] OTAMONGA J P, POTÉ J W. Abandoned mines and artisanal and small-scale mining in Democratic Republic of the Congo (DRC): Survey and agenda for future research [J]. Journal of Geochemical Exploration, 2020, 208: 106394.

[6] KANIKI A T, TUMBA K. Management of mineral processing tailings and metallurgical slags of the Congolese copperbelt: Environmental stakes and perspectives [J]. Journal of Cleaner Production, 2019, 210: 1406−1413.

[7] LUTANDULA M S, MALOBA B. Recovery of cobalt and copper through reprocessing of tailings from flotation of oxidised ores [J]. Journal of Environmental Chemical Engineering, 2013, 1(4): 1085−1090.

[8] WANG Li, JI Bin, HU Yue-hua, LIU Run-qing, SUN Wei. A review on in situ phytoremediation of mine tailings [J]. Chemosphere, 2017, 184: 594−600.

[9] MUIMBA-KANKOLONGO A, BANZA LUBABA NKULU C, MWITWA J M, KAMPEMBA F M, MULELE NABUYANDA M, HAUFROID V, SMOLDERS E, NEMERY B. Contamination of water and food crops by trace elements in the African Copperbelt: A collaborative cross-border study in Zambia and the Democratic Republic of Congo [J]. Environmental Advances, 2021, 6: 100103.

[10] PHIRI T C, SINGH P, NIKOLOSKI A N. The potential for copper slag waste as a resource for a circular economy: A review—Part I [J]. Minerals Engineering, 2022, 180: 107474.

[11] LÈBRE É, CORDER G D, GOLEV A. Sustainable practices in the management of mining waste: A focus on the mineral resource [J]. Minerals Engineering, 2017, 107: 34−42.

[12] FRANKS D M, BOGER D V, CÔTE C M, MULLIGAN D R. Sustainable development principles for the disposal of mining and mineral processing wastes [J]. Resources Policy, 2011, 36(2): 114−122.

[13] HUANG Chu-long, XU Ming, CUI Sheng-hui, LI Zi-rong, FANG Hong-da, WANG Peng. Copper-induced ripple effects by the expanding electric vehicle fleet: A crisis or an opportunity [J]. Resources, Conservation and Recycling, 2020, 161: 104861.

[14] SECK G S, HACHE E, BARNET C. Potential bottleneck in the energy transition: The case of cobalt in an accelerating electro-mobility world [J]. Resources Policy, 2022, 75: 102516.

[15] ZHOU Xiang-yang, ZOU You-lan, ZHAO Guang-jin, YANG Juan. Cycle life prediction and match detection in retired electric vehicle batteries [J]. Transactions of Nonferrous Metals Society of China, 2013, 23(10): 3040−3045.

[16] CRUNDWELL F K, DU PREEZ N B, KNIGHTS B D H. Production of cobalt from copper-cobalt ores on the African Copperbelt—An overview [J]. Minerals Engineering, 2020, 156: 106450.

[17] GAN Yong-gang, DENG Rong-dong, LIU Quan-jun. Surface characteristics, collector adsorption, and flotation response of covellite in oxidizing environment [J]. Transactions of Nonferrous Metals Society of China, 2022, 32(2): 657−667.

[18] FENG Qi-cheng, YANG Wen-hang, WEN Shu-ming, WANG Han, ZHAO Wen-juan, HAN Guang. Flotation of copper oxide minerals: A review [J]. International Journal of Mining Science and Technology, 2022, 32(6): 1351−1364.

[19] TIJSSELING L T, DEHAINE Q, ROLLINSON G K, GLASS H J. Flotation of mixed oxide sulphide copper−cobalt minerals using xanthate, dithiophosphate, thiocarbamate and blended collectors [J]. Minerals Engineering, 2019, 138: 246−256.

[20] SHENGO L M, GAYDARDZHIEV S, KALENGA N M. Assessment of water quality effects on flotation of copper−cobalt oxide ore [J]. Minerals Engineering, 2014, 65: 145−148.

[21] RAO S R, FINCH J A. Base metal oxide flotation using long chain xanthates [J]. International Journal of Mineral Processing, 2003, 69(1/2/3/4): 251−258.

[22] JIA Xiao-dong, SONG Kai-wei, CAI Jin-peng, SU Chao, XU Xiao-hui, MA Yin-yu, SHEN Pei-lun, LIN Dian-wen. Effect of oxygen and sodium sulfide on flotation of cuprite and its modification mechanism [J]. Transactions of Nonferrous Metals Society of China, 2023, 33(4): 1233−1243.

[23] HAN Guang, WEN Shu-ming, WANG Han, FENG Qi-cheng. Enhanced sulfidization flotation of cuprite by surface modification with hydrogen peroxide [J]. Transactions of Nonferrous Metals Society of China, 2021, 31(11): 3564−3578.

[24] YIN Wan-zhong, SUN Qian-yu, LI Dong, TANG Yuan, FU Ya-feng, YAO Jin. Mechanism and application on sulphidizing flotation of copper oxide with combined collectors [J]. Transactions of Nonferrous Metals Society of China, 2019, 29(1): 178−185.

[25] CLARK D W, NEWELL A J H, CHILMAN G F, CAPPS P G. Improving flotation recovery of copper sulphides by nitrogen gas and sulphidisation conditioning [J]. Minerals Engineering, 2000, 13(12): 1197−1206.

[26] KONGOLO K, KIPOKA M, MINANGA K, MPOYO M. Improving the efficiency of oxide copper–cobalt ores flotation by combination of sulphidisers [J]. Minerals Engineering, 2003, 16(10): 1023−1026.

[27] LUTANDULA M S, KITOBO W S, KIME M B,

MAMBWE M P, NYEMBO T K. Mineralogical variations with the mining depth in the Congo copperbelt: Technical and environmental challenges in the hydrometallurgical processing of copper and cobalt ores [J]. Journal of Sustainable Mining, 2020, 19(2): 96−114.

[28] TIJSSELING L T, DEHAINE Q, ROLLINSON G K, GLASS H J. Mineralogical prediction of flotation performance for a sediment-hosted copper–cobalt sulphide ore [J]. Minerals, 2020, 10(5): 474.

[29] PEŠA I. Mining, waste and environmental thought on the central African copperbelt, 1950—2000 [J]. Environment and History, 2022, 28(2): 259−284.

[30] SHENGO L M. Potentially exploitable reprocessing routes for recovering copper and cobalt retained in flotation tailings [J]. Journal of Sustainable Metallurgy, 2021, 7(1): 60−77.

# 采用重选−浮选联合工艺从刚果(金)废石矿中回收铜和钴

汪清清[1,2]，孙 磊[1,2]，曹 杨[1,2]，王 鑫[1,2]，乔 毅[1,2]，向美桃[1,2]，刘国斌[1,2]，孙 伟[1,2]

1. 中南大学 资源加工与生物工程学院，长沙 410083；

2. 中南大学 战略含钙矿物资源清洁高效利用湖南省重点实验室，长沙 410083

**摘 要**：从刚果(金)SICOMINES 矿区废石矿中回收铜和钴金属。通过扫描电镜和能谱分析对矿样进行工艺矿物学分析。结果表明，铜矿物赋存形式多样且粒度不均匀；钴以高度分散的钴土矿形式存在，大量易泥化脉石矿物填充在样品中，造成铜钴矿物分离困难。粒度范围对该铜钴矿样品分选方法的选择具有决定性作用，对于 43~246 μm 粒级的样品，宜采用重选选别，而对于<43 μm 粒级的样品浮选表现出更优异的富集效果。矿样经粗磨分级后，采用重选−浮选的联合方法，可获得铜回收率为 72.83%、钴回收率为 31.13%的精矿产品。

**关键词**：铜钴废石矿；工艺矿物学；预先分级；浮选；重选

**(Edited by Wei-ping CHEN)**